# Automated Segmentation of Coronary Vessel Wall in OCT Imaging

Kai-Pin Tung[1]
k.tung08@imperial.ac.uk
Wen-Zhe Shi[1]
trustswz@gmail.com
Ranil De Silva[2]
r.desilva@imperial.ac.uk
Eddie Edwards[1]
eddie.edwards@imperial.ac.uk
Daniel Rueckert[1]
d.rueckert@imperial.ac.uk

[1] Biomedical Image Analysis Group
Department of Computing
Imperial College London
London, UK

[2] Royal Brompton Hospital
Imperial College London
London, UK

**Abstract**

The aim of this study is to automatically detect the boundary of vessel walls in optical coherence tomography (OCT) sequences. We developed a new method to eliminate guide-wire shadow artifacts and accurately estimate the vessel wall. The estimation of the position of the guide-wire is the key concept for the elimination of guide-wire shadow artifacts. After identification of the artifacts we propose a geometrically-based method which can be applied to OCT cross-section images to remove the artifacts. The segmentation approach is based on a novel combination of expectation maximization (EM) based segmentation and graph cuts (GC) based segmentation. Validation is performed using simulated data and 4 typical in vivo OCT sequences. The comparison against manual expert segmentation demonstrates that the proposed vessel wall identification is robust and accurate.

## 1 Introduction

Optical coherence tomography (OCT) is a light-based imaging technique that provides in vivo high-resolution ($<20\mu m$) images of vessels, including the coronary arteries. This intravascular modality can accurately differentiates the vessel wall, stent struts and the vascular tissue surrounding them. Knowledge about vessel wall properties is like to be valuable in the management of cardiovascular diseases [6]. Recent studies [3, 4] have proposed several methods for detecting the vessel wall and stent strut by analyzing endovascular OCT sequences. However, these algorithms work well only in OCT images without the presence of guide-wire shadow artifacts. If the artifact exists, a region of the vessel wall will be hidden and this will cause inaccurate vessel wall segmentation. An example of guide-wire shadow artifacts can be observed in Fig.1. Therefore, we propose an automatic algorithm for identification of the vessel lumen, enabling the accurate and robust segmentation despite presence of guide-wire artifacts.

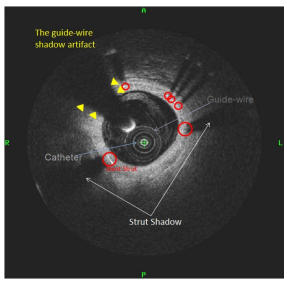


Figure 1: The illustration of an OCT image. The guide-wire shadow artifact is visible from 10 to 11 o'clock position.

# 2 Methods

The proposed approach consists of three components: (a) initial vessel wall detection, (b) elimination of guide-wire shadow artifacts and (c) final vessel wall estimation. A flowchart is shown in Fig.2. A segmentation of the initial vessel wall estimation is obtained using a combination of expectation maximization (EM) and graph cuts (GC). After this initial segmentation, a convex hull approach is used to eliminate the guide-wire shadow artifacts. In the final step, we use an active contour approach to correct and smooth the contour of the vessel wall.

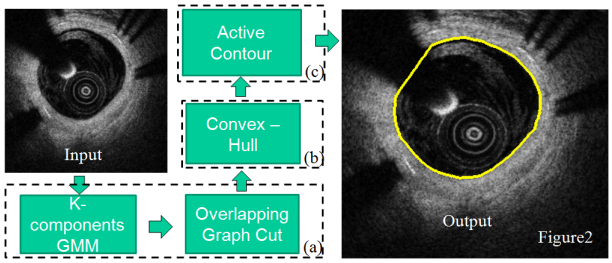


Figure 2: The flowchart of proposed algorithm. OCT image undergoes (a) initial vessel wall detection; (b) artifacts removal and (c) contour correction and smoothing to estimate the hidden region of the vessel wall.

## 2.1 Initial Vessel Wall Detection

We propose a combined EM-based estimation [7] and graph-cut algorithm [1] to obtain an accurate vessel wall segmentation. In our approach, EM-based estimation is used to classify each voxel into binary labels: $L(I_p) = \{L_{background}, L_{foreground}\}$. The EM algorithm consists of two alternating steps: the E-step computes the probability that voxel $v_i$ belongs to label $l$ and the M-step reestimates the model parameters. The iterations of the EM-steps continue until the change of log likelihood is smaller than a predefined threshold.

In order to obtain accurate label of each voxel, we use $k$ components of the Gaussian mixture models (GMM) to assign the probability of each label to a voxel. To avoid mislabeling, we choose multiple components of the GMM to present one label of each voxel. Let $P_{background}$ and $P_{foreground}$ denote the probability that a voxel $v_i$ belongs to label $l$, and we

then obtain the probability of each label as in Eq.1.

$$\begin{aligned} P_{background} &= \sum_{i=1}^{n} P_{li} \\ P_{foreground} &= \sum_{j=n+1}^{k} P_{lj} \end{aligned} \tag{1}$$

where $P_{li}$ and $P_{lj}$ are the probability of the foreground and background label of one component of GMM; $k$ is the total number of components in the GMM and $n$ is the number of components used for the background label estimation.

After the probability of each label of a voxel has been obtained, we then use a graph-cut algorithm to estimate the segmentation of vessel wall. The graph-cut algorithm is energy based functions used for labeling problems. It is composed of a region term and a boundary term. The region term captures the global characteristics of an image and is estimated using the output of the previous EM segmentation step. A coefficient $\lambda$ in region term is used to specify a relative importance of the region term versus the boundary properties term. The boundary term ensures that the labeling $f$ is smooth by penalizing two neighboring labels $f_p$ and $f_q$ if they are different but their intensities are similar.

However, if we formulate our data set in a graph and perform 3D graph cuts (using a 26-neighborhood system), large amount of memory is required to represent the graph. Since this is not feasible on a standard PC, we propose an approach where the 3D graph is divided into several overlapping graphs. We divide a volumetric image set into several overlapping subsets and run the simulation on each subset to obtain the label of each voxel.

In practice, we divide an OCT sequence into the subsets of $p$ frames. Succeeding subsets overlap by $q$ frames to guarantee a consistent segmentation across frames. Figure 3(a) shows the result of the initial vessel wall segmentation. We can clearly notice segmentation errors as a result of the presence of the guide-wire. The next section explains how these segmentation errors can be corrected.

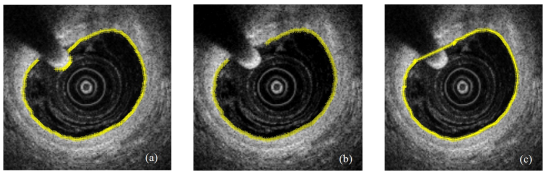


Figure 3: The procedure of proposed method. (a)initial vessel wall detection, (b)elimination of guide-wire artifacts, (c) automatic vessel wall estimation.

## 2.2 Elimination of Guide-Wire Artifacts and Vessel Wall Estimation

The artifacts in the OCT image cause a failure of the boundary detection of the vessel wall that occluded by the guide-wire shadows. To remove the artifacts, we have used a convex hull approach [2]. The first step is to identify the portion of the vessel wall which is affected by the artifacts. From the initial segmentation, it is obvious that the artifacts appear inside of the vessel wall. Thus, it is reasonable to assume that the distances between artifacts and the convex hull of the vessel wall are larger than the distances between the vessel wall points and the convex hull of the vessel wall.

In practice, we construct a set that contains the distances from each point on the vessel wall to the convex hull of the vessel wall. The point $v$ that has the maximum distance can be obtained by Eq. 2.

$$v = argmax(H_{convex}(X))) \tag{2}$$

where $H_{convex}(X)$ is the convex hull of the initial vessel wall segmentation.

We consider the point $v$ as the seed point of an initial artifacts set $S$ and set the vessel wall points connected to $S$ into a neighborhood set $N$. If the distance between a point in the neighborhood set $N$ and the convex hull is larger than the mean distance, we can assume that this point is an erroneous point resulting from the guide-wire shadow and add this point into the artifacts set $S$. We then iterate this process until the artifacts set is not growing. With the identified points, a new vessel wall point set and artifacts point set could be obtained. Figure 3(b) shows the new vessel wall point set.

We then use a deformable approach, active contour [5], to correct the contour of vessel wall and to extrapolate the contour in the area of the guide-wire shadow. The framework of this method attempts to minimize an energy associated to the current contour as a sum of an internal and external energy. An internal energy determines the shape of the contour and an external energy describes the image properties. The new vessel wall point set is used to initialize the active contour model near to the real edges of the vessel. Thus, the vessel wall is precisely segmented (see results in Fig. 3(c)).

## 3 Results and Discussions

Our three-step automatic vessel wall segmentation process has been applied to all four OCT sequences. For the inital vessel wall detection, we divide the OCT sequences into sub-images of 64 frames. Subsequent sub-images share 44 frames in order to guarantee a consistent segmentation across frames. We chose 0.5 as the value of $\lambda$ of the region term weight in the graph cut step. The number of iterations of the active contour model in the final step was set to 100 and the estimated number of points of vessel wall was set to 400. In addition, we chose 0.1 as the parameter to control the convergence of the energy function in the final estimation. Figure 4 shows the results of vessel wall segmentation in all four data sets.

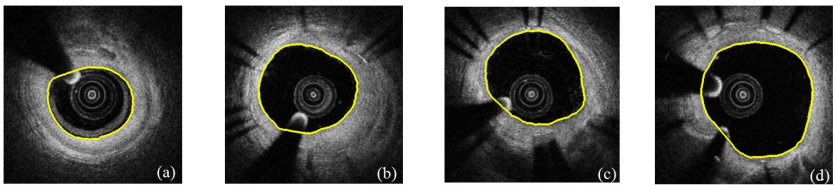


Figure 4: Vessel wall estimation: (a), (b), (c) and (d) show the estimation of the vessel wall in a randomly chosen frame in each data set. Yellow contours are used to indicate the vessel wall without the guide-wire shadow artifact.

To evaluate our results, we computed the accuracy of the segmentation. The accuracy is estimated using the overlap (DICE) of the manual and automatic segmentation as a metric.Table 1 presents measurements of the DICE overlap and the surface distance between EM&GC segmentation and automatic segmentation.

In our proposed method, the average DICE overlap is $0.97\pm0.02$ for the given datasets. Compared with the EM&GC method, our method achieves a high accuracy rate. However, a vessel contour estimation would become inflexible when the artifacts have been removed frame by frame. A possible solution is to extend our contour correction and smoothing method into 3D. The missing region in the current frame maybe correctly display in the neighboring frames. Thus, a 3D estimation could be more consistent and produce more continuous segmentations.

Table 1: The accuracy measurements of the proposed method and the EM&GC algorithm.

| | Dataset 1 | Dataset 2 | Dataset 3 | Dataset 4 |
|---|---|---|---|---|
| Proposed (dice-metric) | 0.98±0.01 | 0.98±0.02 | 0.96±0.03 | 0.97±0.02 |
| EM&GC (dice-metric) | 0.92±0.03 | 0.94±0.04 | 0.88±0.06 | 0.89±0.05 |

# 4 Conclusions

We presented a new fully automated method for the vessel wall detection which uses EM&GC-based segmentation, convex hull detection and active contour models to obtain accurate segmentations. Our method has focused on the images which have guide-wire shadow artifacts and these artifacts would result in inaccurate vessel wall segments. Our method therefore estimates the possible vessel wall position in the region affected by guide-wire shadows and segments the vessel wall accurately.

# 5 Acknowledgements

Dr. de Silva is supported by Imperial College London and NIHR Cardiovascular Disease Biomedical Research Unit at the Royal Brompton and Harefield NHS Foundation Trust.

# References

[1] Y. Boykov, O. Veksler, and R. Zabih. Fast approximate energy minimization via graph cuts. *IEEE Transactions on Pattern Analysis and Machine Intelligence*, 23(11):1222–1239, 2001.

[2] M. de Berg, M. van Kreveld, M. Overmars, and O. Schwarzkopf. *Computational Geometry: Algorithms and Applications*. Springer, 1997.

[3] F. Dubuisson, C. Kauffmann, P. Motreff, and L. Sarry. In vivo oct coronary imaging augmented with stent reendothelialization score. *Medical Image Computing and Computer-Assisted Intervention*, 5761:475–482, 2009. doi: http://dx.doi.org/10.1007/978-3-642-04268-3_59.

[4] S. Gurmeric, G. G. Isguder, S. Carlier, and G. Unal. A new 3-d automated computational method to evaluate in-stent neointimal hyperplasia in in-vivo intravascular optical coherence tomography pullbacks. *Medical Image Computing and Computer-Assisted Intervention*, 5762:776–785, 2009.

[5] M. Kass, A. Witkin, and D. Terzopoulos. Snakes: Active contour models. *International Journal of Computer Vision*, 1(4):321–331, 1988.

[6] J. D. Pearson. Vessel wall interactions regulating thrombosis. *British Medical Bulletin*, 50(4):776–788, 1994.

[7] Y. Zhang, M. Brady, and S. Smith. Segmentation of brain mr images through a hidden markov random field model and the expectation-maximization algorithm. *IEEE Transactions on Medical Imaging*, 20:45 –57, 2001. ISSN 0278-0062.